

# A Damped Ly $\alpha$ Absorption-Line System in an Apparent Void at Redshift 2.38

Leith E. H. Godfrey<sup>A</sup> and Paul J. Francis<sup>A,B</sup>

<sup>A</sup> Research School of Astronomy and Astrophysics, Australian National University, Canberra ACT 0200, Australia

<sup>B</sup> Corresponding author. Email: pfrancis@mso.anu.edu.au

Received 2005 February 16, accepted 2005 June 22

**Abstract:** We study the contents of an apparent void in the distribution of Ly $\alpha$  emitting galaxies at redshift 2.38. We show that this void is not empty, but contains a damped Ly $\alpha$  absorption-line system, seen in absorption against background QSO 2138-4427. Imaging does not reveal any galaxy associated with this absorption-line system, but it contains metals ( $\text{Fe}/\text{H} \sim -1.3$ ), and its large velocity range ( $\sim 180 \text{ km s}^{-1}$ ) implies a significant mass.

**Keywords:** Large Scale Structure of Universe — quasars: individual (2138-4427) — quasars: absorption lines

## 1 Introduction

It is now abundantly clear that high redshift galaxies are as strongly clustered as those in the local universe (e.g. Giavalisco et al. 1998; Steidel et al. 2000). The topology of this clustering is not as clear, but there is some evidence that high redshift galaxies, just like their local descendants, lie in filamentary structures, separated by voids (e.g. Campos et al. 1999; Møller & Fynbo 2001; Palunas et al. 2004; Turnshek et al. 2004).

In the local universe, voids are surprisingly free of galaxies (e.g. Peebles 2001). The few galaxies seen in voids are unusually blue and tend to be centrally concentrated (e.g. Roias et al. 2004, and references therein). Low column density Ly $\alpha$  forest QSO absorption-line systems can also be found in voids (Shull, Stocke, & Penton 1996; Penton, Stocke, & Shull 2004). At higher redshifts, cold dark matter modelling predicts that galaxy biasing should be much stronger than today (e.g. Fry 1996; Bagla 1998; Tegmark & Peebles 1998; Baugh et al. 1999). The *dark matter* underdensity in voids should thus be much less than it is today. One might thus expect to find more or different objects in any voids.

Palunas et al. (2004) mapped an  $80 \times 60 \times 60$  co-moving Mpc region of the high redshift universe, at  $z = 2.38$  (see also Francis et al. 2004). They showed that the distribution of Ly $\alpha$  emitting galaxies was not random. The void probability function was significantly higher than that expected for randomly distributed galaxies on scales of 5–10 Mpc. The signal was dominated by a single large empty region just to the north-west of their field centre.

These voids are deficient in Ly $\alpha$  emitting galaxies, but do they contain anything else? Luckily, a luminous background QSO, LBQS 2138-4427, lies behind the major void. Francis & Hewett (1993) showed that this QSO had

a damped Ly $\alpha$  absorption-line system at redshift 2.383. This redshift places the damped system clearly within the major Palunas et al. void, more than 10 co-moving Mpc from any Ly $\alpha$  emitting galaxies.

Is the line of sight to this QSO really passing through a void, or is the lack of Ly $\alpha$  emitting galaxies close to it an artefact of small number statistics? In Palunas et al. (2004) we generated mock galaxy catalogues with the same total number of Ly $\alpha$  emitting galaxies as were observed. These mock catalogues assumed a random distribution of galaxies, but allowed for differences in exposure time across our field (the QSO is in a region with the above average exposure time). Less than 1% of these random catalogues had no Ly $\alpha$  emitting galaxies within 10 projected co-moving Mpc of the QSO sight line. We therefore tentatively conclude that this sight line is probing a region that is underdense in Ly $\alpha$  emitting galaxies.

In this paper, we show that imaging fails to identify any galaxy candidate that could be associated with this damped Ly $\alpha$  absorption-line system. We present high-resolution spectroscopy which demonstrates, however, that the damped system is substantially enriched with a wide variety of heavy elements. The velocity sub-structure of the damped system also indicates the likely presence of significant mass. This void is thus far from empty.

## 2 Imaging

The area around QSO 2138-4427 was imaged by Palunas et al. (2004), down to a Ly $\alpha$  flux limit of  $1.4 \times 10^{-16} \text{ erg cm}^{-2} \text{ s}^{-1}$ , and down to (AB) broad-band magnitude limits of  $B = 26.2$ ,  $V = 25.3$ ,  $R = 24.0$ , and  $I = 23.8$ . Nothing was seen within 10 arcsec of the QSO in any of these bands: it is an unusually clear sight line. Near-IR imaging was obtained on the nights of

1998 September 6–7, using the CASPIR (Cryogenic Array Spectrometer/Imager) camera on the Siding Spring 2.3-m telescope. A total of 4.5 h exposure time was obtained in the H-band, reaching a (Vega) magnitude limit of  $H=20.5$ . Once again nothing was seen within 10 arcsec of the QSO.

### 3 Spectroscopy

#### 3.1 Observations and Reduction

Our existing spectra of LBQS 2138-4427 (Francis & Hewett 1993) were of too low a resolution and narrow a wavelength coverage to seriously constrain the physical properties of the gas. We therefore re-observed it using the University College London Echelle Spectrograph (UCLES) on the Anglo-Australian Telescope (AAT). Observations were carried out on the nights of 2001 August 20–23 and the total usable integration time was 43 200 s. D’Odorico, Petitjean, & Cristiani (2002) independently obtained high-resolution spectra of this QSO, using the VLT Ultraviolet Visual Echelle Spectrograph (UVES). They kindly allowed us to use their spectrum in this analysis. Both spectra have velocity resolutions corresponding to a Doppler parameter  $b = 6 \text{ km s}^{-1}$ . Where they overlap, the two spectra agree very well.

The data were reduced using standard procedures, and set to the vacuum heliocentric frame. The UVES spectrum has a higher signal-to-noise ratio, and a wider wavelength coverage in the red: it was used for our analysis of most lines. The C $\text{IV}$  doublet, however, was not covered by UVES, so we used the UCLES spectrum.

Absorption-line properties were measured interactively using the XVOIGT program (Mar & Bailey 1995). Upper and lower limits were derived interactively by varying parameters until residuals clearly exceeded the noise. In most cases, possible line blending and/or saturation dominated noise as the major source of uncertainty.

#### 3.2 Results

The damped Ly $\alpha$  system was clearly detected in a wide variety of transitions (Figure 1). Low ionization transitions such as O $\text{I}$  and Mg $\text{II}$  dominated, though a relatively weak detection was made in C $\text{IV}$ .

In the majority of transitions, the line breaks up into about nine sub-components, with relative velocities spanning  $178 \text{ km s}^{-1}$ . Each individual component is spectrally unresolved, or at best marginally resolved. The measured properties of the components are shown in Table 1. The neutral hydrogen content of each individual component cannot be constrained, though the total neutral hydrogen content of the system is  $\log(N(\text{H}\text{I})) = 20.5 \pm 0.1$ . In some cases (C $\text{II}$ , Mg $\text{II}$ ), the inner components blended into a single absorption feature, and consequently an estimate of the column density for each inner component was not possible. However, an upper limit on the combined column density could be determined in these cases. Several ionic transitions did not produce observable absorption features (either due to blending with unassociated lines or to low

column density). For these ions, only upper limits on the column density were possible (assuming that their velocity structure was the same as that of the other transitions). C $\text{IV}$  clearly has a different profile from the other (lower ionization) transitions and was best fit with two components at  $v_{\text{rel}} = -2$  and  $14 \text{ km s}^{-1}$ , each having  $N(\text{CIV}) \sim 10^{14.2} \text{ cm}^{-2}$  with velocity dispersion  $b \sim 10\text{--}20 \text{ km s}^{-1}$ .

#### 3.3 Composition and Physical Properties of the Gas

This system appears to be a very typical damped Ly $\alpha$  system. The predominance of low ionization species and the narrowness of the individual sub-components suggest that they are cool and relatively dense. We modelled a typical low ionization sub-component, using Gary Ferland’s CLOUDY code (Ferland 1996), and assuming photoionization of a uniform density, plane parallel slab by a typical diffuse UV background (Haardt & Madau 1996; Scott et al. 2000; Simcoe, Sargent, & Rauch 2004). The line ratios are consistent with the hydrogen being predominantly neutral (Dessauges-Zavadsky et al. 2004), though we are unable to completely rule out partial hydrogen ionization (e.g. Prochaska et al. 2002; Vladilo et al. 2001; Izotov, Schaerer, & Charbonnel 2001). The modelling suggests densities of  $\sim 10^{-3}\text{--}10^{-1} \text{ cm}^{-3}$  and a temperature of  $\sim 10^4 \text{ K}$ . If we assume that the gas in these components is mostly neutral, we infer mean metallicities [Fe/H], [Si/H], [O/H], and [Al/H] all of  $\sim -1.3$ . This is compared with the mean metallicity of  $\langle [\text{Zn}/\text{H}] \rangle \approx -1.15 \pm 0.15 \text{ dex}$  for DLAs at  $z > 1.5$  (Prochaska & Wolfe 1999).

### 4 Conclusion

We conclude that this apparent void is not empty: it contains a very typical damped Ly $\alpha$  absorption-line system. The non-detection of any galaxy counterpart in our imaging is very consistent with this: only a tiny fraction of damped systems have identifiable counterparts (e.g. Bouché & Lowenthal 2004, and references therein). The galaxy counterparts presumably either lie under the point-spread function of the background QSO or are below the detection limits.

The absorption-line spectra clearly show, however, that the gas in the damped system is condensed into cool cloudlets, and that it is enriched in a wide variety of elements. The large velocity dispersion between the components further suggests that quite a large mass may be present.

We are not implying that all damped Ly $\alpha$  systems arise in voids. The inter-relationship of damped systems and galaxies is clearly complex. On large scales, Lyman-break galaxies and damped systems seem, on average, to trace each other (Bouché & Lowenthal 2004). In our field, there are two additional damped Ly $\alpha$  absorption-line systems seen in the spectra of two different background QSOs. One of these lies within an apparent proto-cluster (Francis & Williger 2004), while the other lies on the fringe of the major void (Francis, Wilson, & Woodgate 2001). To add to the complexity, we are delineating the void using Ly $\alpha$  emitting galaxies. Due to its high optical depth and easy

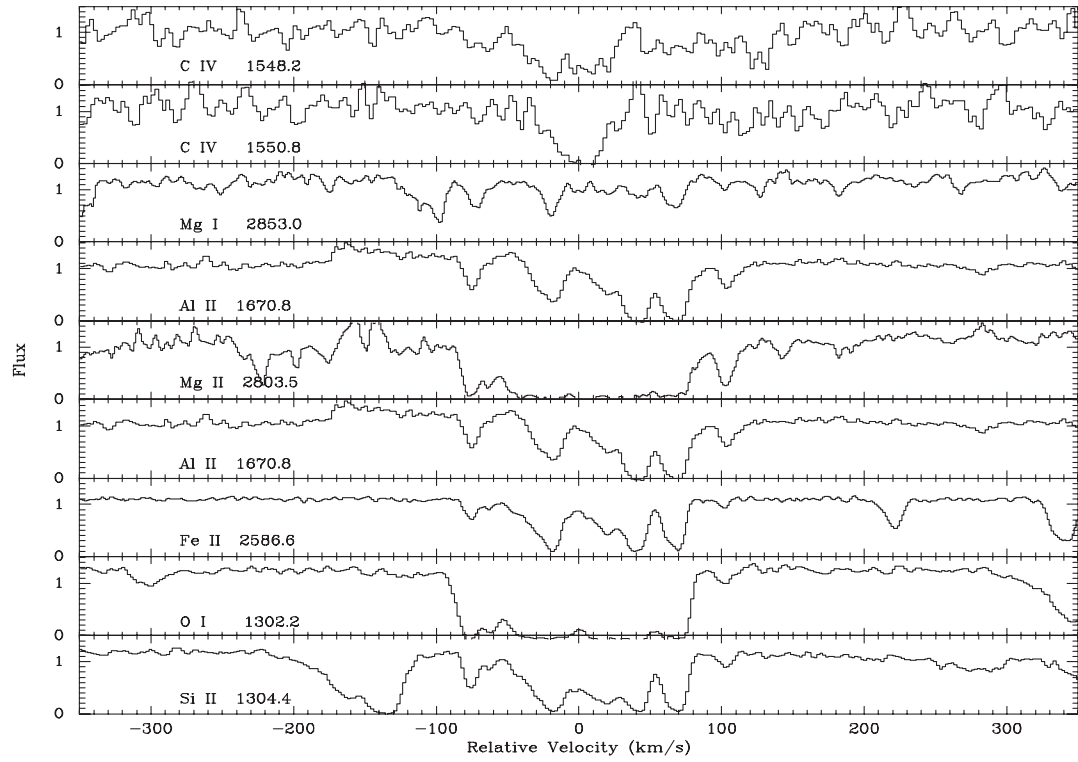


**Figure 1** Spectra of the nine different transitions. The C IV data are from the UCLES spectrum, and the others are from the UVES spectrum. Velocities are relative to a nominal redshift of 2.383.

**Table 1.** Measured parameters of low-ionization sub-components

Property	Sub-component								
	1	2	3	4	5	6	7	8	9
$v_{\text{rel}}^a$ (km s $^{-1}$ )	-74	-59	-42	-37	-16	21	43	68	104
$b^b$ (km s $^{-1}$ )	<6	<6	<7	<8	<10	<12	<10	<9	<6
	Log(column density) (cm $^{-2}$ )								
C I	<12.6	<12.7	<12.7	<12.7	<12.7	<12.7	<12.7	<12.7	<12.7
C II	14.4 $^{+0.9}_{-0.4}$	14.2 $^{+0.6}_{-0.6}$	...	...	...	...	...	...	13.8 $^{+1.2}_{-0.2}$
N I	<13.3	<13.7	<13.5	<13.7	<14.5	<14.1	<14.5	<14.0	<13.6
O I	15.0 $^{+1.9}_{-0.5}$	14.4 $^{+1.6}_{-0.2}$	14.2 $^{+1.7}_{-0.2}$	14.6 $^{+3.0}_{-0.4}$	14.9 $^{+1.0}_{-0.1}$	15.0 $^{+1.8}_{-0.2}$	15.2 $^{+1.8}_{-0.6}$	15.6 $^{+1.3}_{-0.6}$	13.1 $^{+0.3}_{-0.3}$
Mg I	11.6 $^{+0.3}_{\text{inf}}$	11.1 $^{+0.3}_{\text{inf}}$	<11.2	<11.2	12.0 $^{+0.2}_{-0.2}$	11.5 $^{+0.3}_{-0.2}$	11.6 $^{+0.3}_{-0.2}$	11.9 $^{+0.2}_{-0.2}$	11.4 $^{+0.4}_{-0.6}$
Mg II	13.4 $^{+0.8}_{-0.5}$	13.0 $^{+0.5}_{-0.3}$	...	...	...	...	...	...	13.1 $^{+0.6}_{-0.3}$
Al III	12.1 $^{+0.4}_{-0.2}$	11.5 $^{+0.2}_{-0.5}$	11.0 $^{+0.5}_{-1.0}$	11.9 $^{+0.5}_{-0.3}$	12.4 $^{+0.2}_{-0.1}$	12.4 $^{+0.3}_{-0.2}$	13.4 $^{+1.6}_{-0.5}$	13.3 $^{+1.6}_{-0.5}$	12.0 $^{+1.1}_{-0.2}$
Si I	<12.0	<12.0	<12.0	<12.0	<12.0	<12.0	<12.0	<12.0	<12.0
Si II	13.9 $^{+1.6}_{-0.6}$	12.8 $^{+0.8}_{-0.2}$	13.0 $^{+0.2}_{-0.3}$	13.0 $^{+0.4}_{-0.3}$	14.0 $^{+0.2}_{-0.1}$	14.0 $^{+0.2}_{-0.1}$	14.4 $^{+0.8}_{-0.6}$	13.9 $^{+0.3}_{-0.4}$	13.1 $^{+0.2}_{-0.1}$
Si III	<12.6	<12.3	<12.7	<12.5	<15.4	<14.8	<13.0	<16.3	<13.6
Si IV	<12.4	<12.4	<12.2	<12.3	<12.4	<12.4	<12.2	<12.2	<12.5
Si	<12.7	<12.7	<12.7	<12.7	<12.7	<12.7	<12.7	<12.7	<12.7
Cr II	<12.0	<12.0	<12.0	<12.1	<12.6	<12.1	<12.5	<12.4	<12.2
Fe I	13.2 $^{+0.1}_{-0.2}$	12.9 $^{+0.1}_{-0.3}$	12.9 $^{+0.4}_{-0.2}$	13.2 $^{+0.4}_{-0.2}$	14.2 $^{+1.6}_{-0.4}$	13.7 $^{+0.3}_{-0.2}$	14.0 $^{+2.3}_{-0.1}$	14.0 $^{+0.6}_{-0.1}$	12.4 $^{+0.3}_{-0.1}$
Fe II	<14.0	<13.5	<13.9	<14.3	<14.1	<14.1	<14.1	<13.8	<13.0
Ni II	<12.6	<12.6	<12.6	<12.6	<13.0	<12.4	<12.8	<12.6	<12.6
Zn II	<11.3	<11.1	<11.2	<11.2	<11.6	<11.5	<11.5	<11.4	<11.4

<sup>a</sup> Velocity of component relative to  $z = 2.383$ .

<sup>b</sup> Velocity dispersion of individual sub-component.

destruction by dust, Ly $\alpha$  emission is not expected to correlate straightforwardly with any easily modellable property of a galaxy, such as its mass or star formation rate — their distribution is thus hard to model. In addition, the apparent void is only 99% significant.

We tentatively conclude, however, that at least one damped system lies within an apparent void, and that this damped system contains significant metal enrichment, and is probably associated with considerable mass.

### Acknowledgment

We wish to thank Cedric Ledoux for making the UVES spectrum available to us.

### References

- Bagla, J. S. 1998, *MNRAS*, 299, 417
- Baugh, C. M., Benson, A. J., Cole, S., Frenck, C. S., & Lacey, C. G. 1999, *MNRAS*, 305, L21
- Bouché, N., & Lowenthal, J. D. 2004, *ApJ*, 609, 513
- Campos, A., Yahil, A., Windhorst, R. A., Richards, E. A., Pascarelle, S., Impey, C., & Petry, C. 1999, *ApJL*, 511, L4
- D'Odorico, V., Petitjean, P., & Cristiani, S. 2002, *A&A*, 390, 13
- Dessauges-Zavadsky, M., Calura, F., Prochaska, J. X., D'Odorico, S., & Matteucci, F. 2004, *A&A*, 416, 79
- Ferland, G. J. 1996, *HAZY*, a Brief Introduction to *CLOUDY*, University of Kentucky Department of Physics and Astronomy Internal Report
- Francis, P. J., & Hewett, P. C. 1993, *AJ*, 106, 2587
- Francis, P. J., Palunas, P., Teplitz, H. I., Williger, G. M., & Woodgate, B. E. 2004, *ApJ*, 614, 75
- Francis, P. J., & Williger, G. M. 2004, *ApJ*, 602, 77
- Francis, P. J., Wilson, G. M., & Woodgate, B. E. 2001, *PASA*, 18, 64
- Fry, J. N. 1996, *ApJ*, 461, 65
- Giavalisco, M., Steidel, C. C., Adelberger, K. L., Dickinson, M. E., Pettini, M., & Kellogg, M. 1998, *ApJ*, 503, 543
- Haardt, F., & Madau, P. 1996, *ApJ*, 461, 20
- Izotov, Y. I., Schaerer, D., & Charbonnel, C. 2001, *ApJ*, 549, 878
- Mar, D. P., & Bailey, J. G. 1995, *PASA*, 12, 239
- Møller, P., & Fynbo, J. U. 2001, *A&A*, 372, L57
- Palunas, P., Teplitz, H. I., Francis, P. J., Williger, G. M., & Woodgate, B. E. 2004, *ApJ*, 602, 545
- Peebles, P. J. E. 2001, *ApJ*, 557, 495
- Penton, S. V., Stocke, J. T., & Shull, J. M. 2004, *ApJS*, 152, 29
- Prochaska, J. X., Howk, J. C., O'Meara, J. M., Tytler, D., Wolfe, A. M., Kirkman, D., Lubin, D., & Suzuki, N. 2002, *ApJ*, 571, 693
- Prochaska, J. X., & Wolfe, A. M. 1999, *ApJ*, 121, 369
- Roias, R. R., Vogeley, M. S., Hoyle, F., & Brinkmann, J. 2004, *ApJ*, 617, 50
- Scott, J., Bechtold, J., Dobrzycki, A., & Kulkarni, V. P. 2000, *ApJS*, 130, 67
- Shull, M. J., Stocke, J. T., & Penton, S. 1996, *AJ*, 111, 72
- Simcoe, R. A., Sargent, W. L. W., & Rauch, M. 2004, *ApJ*, 606, 92
- Steidel, C. C., Adelberger, K. L., Shapley, A. E., Pettini, M., Dickinson, M., & Giavalisco, M. 2000, *ApJ*, 532, 170
- Tegmark, M., & Peebles, P. J. E. 1998, *ApJL*, 500, L79
- Turnshek, D. A., Rao, S. M., Nestor, D. B., Vanden Berk, D., Belfort-Mihalyi, M., & Monier, E. M. 2004, *ApJL*, 609, L53
- Vladilo, G., Centurión, M., Bonifacio, P., & Howk, J. C. 2001, *ApJ*, 557, 1007